

Infrared spectroscopy of matrix-isolated polycyclic aromatic compounds and their ions. 7. Phenazine, a dual substituted polycyclic aromatic nitrogen heterocycle

A.L. Mattioda^{a,b,*}, D.M. Hudgins^a, C.W. Bauschlicher Jr.^a, L.J. Allamandola^a

^a NASA Ames Research Center, MS245-6 Moffett Field, CA 94035, USA

^b SETI Institute 515 N. Whisman Road, Mountain View, CA 94043, USA

Received 30 November 2004; received in revised form 30 March 2005; accepted 30 March 2005

Abstract

The matrix-isolation technique has been employed to measure the mid-infrared spectra of phenazine ($C_{12}H_8N_2$), a dual substituted polycyclic aromatic nitrogen heterocycle (PANH), in the neutral, cationic and anionic forms. The experimentally measured band frequencies and intensities are tabulated and compared with their calculated values as well as those of the non-substituted parent molecule, anthracene. The theoretical band positions and intensities were calculated using both the 4-31G as well as the larger 6-31G* basis sets. A comparison of the results can be found in the tables. The spectroscopic properties of phenazine and its cation are similar to those observed in mono-substituted PANHs, with one exception. The presence of a second nitrogen atom results in an additional enhancement of the cation's total integrated intensity, for the $1500\text{--}1000\text{ cm}^{-1}$ ($6.7\text{--}10\text{ }\mu\text{m}$) region, over that observed for a mono-substituted PANH cation. The significance of this enhancement and the astrobiological implications of these results are discussed.

© 2005 COSPAR. Published by Elsevier Ltd. All rights reserved.

Keywords: Phenazine; PANHs; PAHs; Polycyclic aromatic hydrocarbons; Nitrogen heterocycles; Unidentified infrared bands

1. Introduction

Due to their increasing importance in the field of astrophysics, polycyclic aromatic hydrocarbons (PAHs) have been the focus of numerous fundamental molecular and spectroscopic investigations during the past decade. This is due in a large part to the ubiquitous interstellar infrared emission features, which demonstrates the presence of this class of compounds in a wide variety of astronomical objects (Cox and Kessler, 1999). Over the past few years evidence has been building that these interstellar PAHs contain nitrogen within their ring system (Peeters et al., 2003; Mattioda et al., 2003; Hudgins and Allamandola, 2004; Hudgins et al., 2005). Addi-

tional support for the existence of extraterrestrial polycyclic aromatic nitrogen heterocycles (PANHs) comes from their detection in meteorites (Stoks and Schwartz, 1982; Pizzarello, 2001). PANHs are also believed to be a component of Titan's haze (Ricca et al., 2001). The presence of abiotically produced aromatic nitrogen heterocycle molecules throughout the interstellar medium is of particular astrobiological interest because these types of molecule are involved in many biological processes. If PANHs are indeed ubiquitous throughout the interstellar medium, they should be universally available to habitable bodies (Kuan et al., 2003).

To increase the amount of astrophysically relevant spectroscopic data available for these types of species we have measured the IR spectra of neutral as well as positively and negatively charged phenazine ($C_{12}H_8N_2$). Phenazine is a three ring PAH similar in

* Corresponding author. Tel.: +1 650 604 1075; fax: +1 650 604 6779.
E-mail address: amattioda@mail.arc.nasa.gov (A.L. Mattioda).

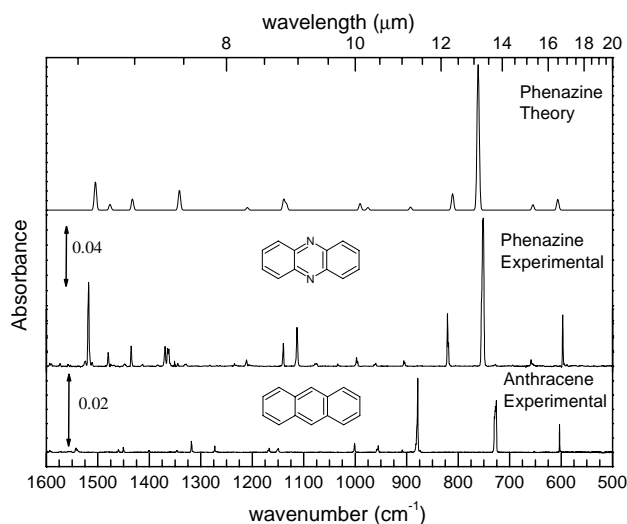


Fig. 1. Comparison of the experimental (bottom) and theoretical (top) spectra for phenazine and the experimental spectrum of anthracene isolated in an argon matrix. All spectra have been normalized to 1×10^{16} molecular species. The theoretical spectrum shown was determined using the 4-31G basis set result.

structure to anthracene ($C_{14}H_{10}$), with the exception that the central carbon atoms have been replaced with nitrogen. Both structures are shown in Fig. 1. Phenazine shares some structural similarities with a biologically important class of molecules known as flavins.

2. Experimental and theoretical methods

2.1. Experimental

The matrix isolation infrared spectroscopy techniques employed in these studies have been described in detail previously (Hudgins and Allamandola, 1995; Hudgins and Sandford, 1998) and will be summarized here only briefly. Matrix-isolated phenazine samples were prepared by vapor co-deposition of the species of interest with an overabundance of argon onto a 14K CsI window suspended in a high-vacuum chamber ($p < 10^{-8}$ Torr). The samples were vaporized from heated Pyrex tubes while argon was admitted through an adjacent length of copper tubing cooled by liquid nitrogen, $N_2(l)$. Deposition temperature for phenazine was 50 °C. Estimates based on the characteristic band intensities of PAHs and the calibrated argon deposition rate place the Ar/phenazine ratio in these experiments in excess of 1000/1 (Hudgins and Sandford, 1998). The phenazine sample was obtained from the National Cancer Institute's Chemical Carcinogen Reference Standard Repository operated by the Midwest Research Institute. Although the sample is of unspecified purity, the absence of any notable discrepant spectral features between the theoretical and experimental spectra indicate impurity levels are no more than a few percent.

Spectra from 6000 to 500 cm^{-1} were measured on either a Nicolet 740 or a Digilab Excalibur FTS 4000 FTIR spectrometer using a KBr beam splitter and $N_2(l)$ -cooled MCT detector. Each spectrum represents a co-addition of between 500 and 1024 scans at a resolution of 0.5 cm^{-1} . This level of resolution is critical for detecting ion bands which fall near the position of a neutral band, whereas the number of scans was chosen to optimize both the signal-to-noise as well as time requirements of each experiment. Integrated intensities ($\int \tau dv$) for individual bands were determined using the WinIR Pro (Digi-Lab) spectrometer control/data analysis software package provided by Digi-Lab. Absolute intensities ($A \equiv \int \tau dv/N$, where τ is the absorbance and N is the density of absorbers in molecules/ cm^2) for the experimentally measured neutral phenazine bands were determined using the theoretically calculated values as follows. The calculated intensities for all bands between 1600 and 500 cm^{-1} were summed to obtain the total absorption intensity over this region. This range was chosen to exclude the contributions of the far-infrared bands ($\nu < 500\text{ cm}^{-1}$) that were not measured in this experiment, the CH stretching region, whose intensities are substantially overestimated by the calculations (Bauschlicher and Langhoff, 1997; Hudgins and Sandford, 1998) and any in-plane CC and CH bending modes which blend with overtone/combination bands in the experimental data. The total theoretically calculated absolute intensity ($\sum A^{\text{thy}}$) was then distributed over the experimental bands (A^{exp}) on the basis of the fractional contribution of each band ($I_{\text{rel},i}^{\text{exp}}$) to the total 1600– 500 cm^{-1} absorption ($I_{\text{rel}}^{\text{exp}}$) in the experimental spectrum:

$$A_i^{\text{exp}} = \left[\sum_{1600 \geq \nu \geq 500} A^{\text{thy}} \right] \frac{I_{\text{rel},i}^{\text{exp}}}{\sum_{1600 \geq \nu \geq 500} I_{\text{rel}}^{\text{exp}}} \quad (1)$$

This method takes advantage of the fact that, although there may be band-to-band variability in the accuracy of the calculated intensity, the total intensity is generally accurate to 10–20%, excluding the C–H stretching region.

Phenazine cations were generated by in situ vacuum ultraviolet photolysis of the matrix-isolated neutral phenazine. This was accomplished with the combined 120 nm Lyman- α (10.1 eV) and the 160 nm molecular hydrogen emission bands (centered around 7.8 eV) from a microwave powered discharge in a flowing H_2 gas mixture at a dynamic pressure of 150 mTorr. Comparison of the pre-photolysis neutral spectrum to that measured after photolysis permitted identification of phenazine ion features (Hudgins et al., 2000). To confirm the attribution of a photoproduct band to the phenazine cation, parallel experiments were conducted in which the argon matrix was doped with an electron acceptor, once with NO_2 and once with CCl_4 , at a concentration of approx-

imately 1 part in 1200. The presence of this electron acceptor quenches the formation of anions and enhances the production of cations. For a particular photoproduct band to be assigned to the cation, it must grow in the presence of the electron acceptor and do so in fixed proportion to the other bands attributed to the cation.

In general, the intensities of the bands corresponding to the PAH ions peak after 4–8 min of photolysis and then remain essentially constant or fall off slightly upon further photolysis. This behavior is consistent with that observed previously for all of the PAHs we have studied to date. Rogue photoproduct bands were not common in these phenazine experiments, numbering 2–4 when present. Most common were the 904 cm^{-1} HAr_2^+ , and 1589 cm^{-1} bands. These appeared moderately strong in a number of experiments. Other weak photoproduct bands at 1388 and 1104 (HO_2^+), and 1039 cm^{-1} (O_3) appeared in several experiments. Bands attributable to trace amounts of H_2O , CO_2 and possibly CO were initially present in some experiments. We have no evidence for phenazine decomposition upon photolysis, or other photoproduct bands, a result consistent with the good agreement between the theoretical and experimental spectra of neutral phenazine mentioned above.

Assuming that all neutral phenazine molecules that disappear are converted into ions, we can derive an upper limit to the ionization efficiency by measuring the percent decrease in the integrated areas of the neutral bands that accompany photolysis. Phenazine demonstrated an upper ionization limit of 11% in both the Ar and Ar/ NO_2 matrix. This value is in line with the ionization limits demonstrated by singly substituted PANH molecules (Mattioda et al., 2003). For presentation purposes only, the data have been baseline corrected, data in the cation and anion figures were obtained by subtracting off the remaining fraction of the neutral bands, using the Win-IR software package (Digi-Lab). No further data reduction was necessary. All numerical values were obtained from the original (unaltered) data.

2.2. Theoretical

All calculations were performed using the Gaussian98 program (Frisch et al., 1998). For the species treated here, the geometries were optimized and the harmonic frequencies computed using density functional theory (DFT). Specifically, the hybrid B3LYP (Stephens et al., 1994; Becke, 1993) functional was utilized in conjunction with the 4-31G as well as the larger 6-31G* basis sets (Frisch et al., 1984). Calibration calculations, (Bauschlicher and Langhoff, 1997) which have been carried out for selected systems, show that a single scale factor of 0.958 brings the B3LYP harmonic frequencies computed using the 4-31G basis set into agreement with the experimental fundamental frequencies, while scaling

factors of 0.9588 (CH stretching modes) and 0.9733 (non-CH stretching modes) are required to bring the 6-31G* basis set into agreement. While previous work has confirmed the use of the 4-31G basis set for PAH molecules, the comparison of the two basis was performed to determine if the B3LYP/4-31G results are still of sufficient accuracy to allow a critical evaluation of the dual nitrogen substituted PAH results. Calibration calculations also show that the computed B3LYP/4-31G intensities are accurate except for CH stretches which are, on average, about a factor of 2 larger than those determined in the matrix studies (Bauschlicher and Langhoff, 1997; Hudgins and Sandford, 1998). Although the gas-phase data are very limited, it appears that the gas-phase intensities, across the spectrum, tend to lie between the matrix and B3LYP values (Schlemmer et al., 1994; Cook and Saykally, 1998; Wagner et al., 2000; Piest et al., 1999; Piest et al., 2001, Oomens et al., 2000). It has also been observed that when two bands of the same symmetry are close in energy, their relative intensities are sensitive to the level of theory, but the sum of their intensities is reliable.

3. Results and discussion

3.1. Neutral phenazine

The infrared spectra of phenazine and anthracene are provided in Fig. 1 with the band positions and intensities in Table 1. As indicated in Table 1, the infrared spectrum of neutral phenazine agrees with the previous experimental studies of Neto et al. (1964), Durnick and Wait (1972), Garrison et al. (1982) and Stammer and Taurinus (1963).

The agreement between the theoretical and experimental results is good. Frequencies predicted by both the 4-31G and the larger 6-31G* basis sets are, on average, within 1% (10 cm^{-1}) of the experimentally measured values. However, the variation between the measured and calculated band intensities is larger, exhibiting average differences around 50% for both basis sets, with one exception. The experimentally measured band at 1344.9 cm^{-1} exhibits an integrated intensity of 0.9 km/mol , compared to the predicted values of 21.0 and 23.8 km/mol for the 4-31G and 6-31G* basis sets. However, there are a number of experimental bands between 1392 and 1369 cm^{-1} , which have no theoretical counterpart but are present in the earlier experimental studies as well. Summing the intensities of these bands results in an $A \cong 25\text{ km/mol}$, close to the theoretically predicted values of 21 and 23 km/mol . Thus, the overall agreement between theory and experiment for most of the individual bands in the neutral molecule is good, regardless of the size of the basis set.

Table 1

Theoretical and experimental band positions (ν), relative (RI) and integrated (km/mol) intensities and symmetry assignments (Sym) for neutral phenazine and experimental band positions for neutral anthracene

Phenazine neutral molecule													Anthracene				
Experiment					Reference	Theory			Experiment vs. theory						ν (cm^{-1})	RI	A
ν (cm^{-1})	λ (μm)	RI	A	Comment		4-31G Basis set		Sym	6-31G* basis set		4-31G basis set		6-31G* basis set				
					ν (cm^{-1})	A	ν (cm^{-1})		A	$\Delta\nu$ (%)	ΔA (%)	$\Delta\nu$ (%)	ΔA (%)				
596.9	16.75	0.13	15.7		1, 2, 3	606.5	11.3	B2U	594.9	14.8	1.59	27.8	0.34	6.1	468	0.20	16.9
658.0	15.20	0.01	1.7		1, 2, 4	654.7	5.9	B1U	648.7	6.3	0.50	243.0	1.42	265.5	602.9	0.09	7.8
752.4	13.29	1.00	124.2	Side band 750.7, shoulder 754.8	1, 2, 3, 4	761.2	153.3	B3U	753.6	121.1	1.17	23.4	0.16	2.5	725.6	1.00	84.3
820.8	12.18	0.17	21.3	Side bands 818.7, 816.4	1, 2, 3, 4	810.9	17.4	B2U	817.5	17.0	1.22	18.3	0.41	20.2			
905.5*, 903.7	11.04, 11.07	0.02	2.4		1, 2, 4	892.5	3.2	B1U	890.8	3.5	1.43	34.8	1.62	45.3	878.3	0.77	66.2
960.0	10.42	0.01	1.7	Complex with bands 963.3, 961.6	1, 2, 4	975.4	2.7	B3U	951.0	1.3	1.60	62.2	0.94	19.6	906.8	0.01	0.8
997.4*, 995.2	10.02, 10.05	0.04	4.4		1, 2, 4	990.5	7.0	B2U	1000.2	5.4	0.69	59.2	0.28	22.8	954.9	0.07	5.9
1078.3	9.27	0.02	2.3	Broad complex with 1075.2	1, 2, 4										1000.9	0.08	6.6
1113.4	8.98	0.16	19.6	Shoulders 1112.2, 1116.2	1, 2, 3, 4	1133.8	6.8	B2U	1132.2	10.2	1.83	65.5	1.69	48.3			
1139.5	8.78	0.07	8.6	Shoulder 1140.7	1, 2, 3, 4	1138.8	11.4	B1U	1138.1	12.0	0.06	33.2	0.12	40.4	1149.2	0.07	5.9
1211.3	8.26	0.02	2.8		1, 2, 4	1209.5	2.8	B2U	1227.0	0.0	0.14	2.0	1.30	100.0	1166.9	0.05	4.2
1329.5	7.52	0.01	1.6	Broad complex	1, 2, 4										1272.5	0.06	5.1
1344.9	7.44	0.01	0.9			1341.5	21.0	B2U	1356.9	23.8	0.25	2166.4	0.89	2466.8	1318.1	0.10	8.4
1362.0*	7.34	0.06	7.9	Side band 1359.3	1, 2, 4										1345.6	0.02	1.7
1364.8	7.33	0.06	6.9		1, 2, 4												
1369.2	7.30	0.08	9.8		2												
1435.2	6.97	0.06	7.5		1, 2, 3, 4	1432.8	11.8	B2U	1441.8	8.5	0.17	57.0	0.46	12.4			
1448.2	6.90	0.01	1.8		1										1450.5	0.04	3.4
1480.0	6.76	0.04	5.2		1	1476.4	6.2	B1U	1482.4	5.6	0.24	18.4	0.17	8.4	1460	0.03	2.5
1510.6	6.62	0.01	1.5		2												
1517.8	6.59	0.32	39.5	Shoulder 1516.0, Side band 1519.3	1, 2, 3, 4	1504.7	29.7	B2U	1530.2	33.3	8.63	24.8	0.82	15.7			
1523.8	6.56	0.02	2.1	Doublet with 1525.0	1										1542	0.08	6.6
															1610.5	0.02	1.7
															1627.8	0.04	3.4
1624.1	6.16	0.11	13.1	Contribution from water band	1, 2, 4	1623.5	4.6	B1U							1675	0.03	2.5
1710.5	5.85	0.01	1.8		1, 2, 4										1707.2	0.04	3.4
															1738.3	0.02	1.7
															1765.4	0.04	3.4
															1780	0.01	0.8
															1796.7	0.05	4.2
															1815.8	0.03	2.5
															1844.1	0.01	0.8
															1903.8	0.02	1.7
1936.5	5.16	0.02	2.5	Side bands 1939.2, 1942.5	1,4										1918.3	0.03	2.5
1957.0	5.11	0.03	3.4	Complex with 1959.1, 1962.1	1, 2, 4										1938.1	0.06	5.1
3025, 3051, 3080, 3094		0.29	35.6		1, 2, 4	3061, 3074, 3091, 3095	113.6	B1U, B2U, B1U, B2U	3058, 3070, 3085, 3088	98.8					2979, 3012, 3032, 3065		
															3106, 3218, 3136	1.60	138.5

(continued on next page)

Table 1 (continued)

Experiment	Reference				Theory				Experiment vs. theory				Anthracene			
	λ (μm)	RI	A	Comment	4-31G Basis set ν (cm^{-1})	Sym	6-31G* basis set ν (cm^{-1})	A	4-31G basis set $\Delta\nu$ (%)	ΔA (%)	6-31G* basis set $\Delta\nu$ (%)	ΔA (%)	ν (cm^{-1})	RI	A	
Previous PANH results			171.4	Sum 500–1000			200.9	169.4							188.5	
Singly substituted			76.5 0.4	Sum 1000–1500 Ratio 1000–1500/500–1000			89.7 0.4	60.1 0.4							31.2 0.2	
PANH/PAH (0.90)			0.90	Phenazine/anthracene 500–1000			1.1	0.9								
PANH/PAH (2.14)			2.5	Phenazine/anthracene 1000–1500			2.9	1.9								

Differences between theoretical and experimental values are provided as percent difference ($\Delta\%$). Average differences are for the 500–1500 cm^{-1} range. Bands below 1% of the max are not included in this table.

1. Neto et al. (1964).

2. Durnick and Wait (1972).

3. Garrison et al. (1982).

4. Stammer and Taurins (1963).

Bands below 1% of the max are not included in this table.

* Indicates major band of a multiplet.

Comparison of neutral phenazine with anthracene (Fig. 1), the unsubstituted PAH analog, reveals two items of interest. As discussed in Mattioda et al. (2003) and Garrison et al. (1982) with singly substituted PANHs, the presence of nitrogen in the structure induces a global enhancement of the features in the 1600–1000 cm^{-1} region. The modes that fall in this region correspond to the aromatic CN and CC stretching as well as the CH in-plane bending modes. This behavior is similar to that observed upon ionization (Szczepanski et al., 1992 and Hudgins et al., 1994) of a non-substituted PAH. For instance, the sum of the total vibrational intensity in the 6.7–10 μm range (1500–1000 cm^{-1}) for neutral phenazine is 76.5 km/mol, which is double that observed for neutral anthracene (see Table 1). However, this is in excellent agreement with that observed for singly substituted PANHs, but not quite the 20-fold enhancement encountered upon ionization of a non-substituted PAH (Mattioda et al., 2003). Thus, the presence of an additional nitrogen in the aromatic structure does not appear to increase the enhancement observed in singly substituted, neutral PANHs.

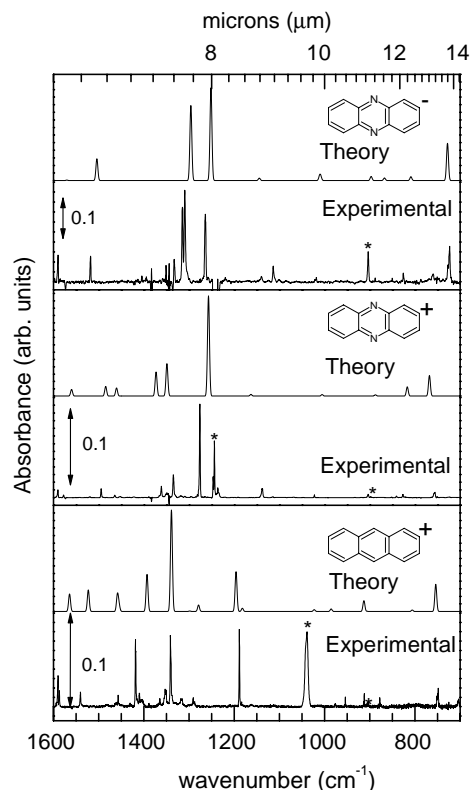


Fig. 2. Mid-infrared spectra of the phenazine anion and cation isolated in an argon (anion) and argon/ NO_2 (cation) matrix at 14 K. The corresponding spectra for anthracene are shown for reference. The neutral spectrum of anthracene, recorded in our laboratory, is in good agreement with that of Szczepanski and Vala (1993). The bands marked by an asterisk (*) are due to impurity photoproducts. All spectra have been normalized to 1×10^{16} molecular species. The theoretical spectra were determined using the 4-31G basis set results.

Calculations performed for the Mattioda et al. (2003) investigation indicated that modes dominated by CN stretching and CNC in-plane bending tend to fall in the 1100–1000 cm^{-1} region, although such bands tended to be weak in intensity. One would expect the presence of an extra nitrogen would increase the intensity of the CN stretching and CNC in-plane bending modes. Indeed, the neutral spectrum of phenazine displays two fairly intense bands at 1113.4 (9.0 μm) and 1139.5 cm^{-1} (8.8 μm).

Within the context of the interstellar emission spectrum, bands at positions such as these would contribute to the long wavelength wing of the pedestal under the interstellar 6.8/7.7/8.6 μm features. If further studies show that vibrational bands falling in this region only occur in PANHs, the long wavelength emission in the pedestal, and perhaps even the 8.6 μm feature, would then be another indicator of interstellar nitrogenated aromatic species.

The presence of an additional nitrogen atom does not appear to have any additional influence on the CH out-of-plane bending region (10–20 μm) over that already observed in a singly substituted PANH.

3.2. Phenazine cation

The spectra of the argon/ NO_2 matrix-isolated phenazine cation and argon matrix-isolated anthracene cation are compared in Fig. 2, along with the 4-31G theoretical results. The observed band positions and intensities of the phenazine cation are reported and compared to their calculated values as well as the values for the anthracene cation in Table 2.

Inspection of Table 2 reveals frequency discrepancies between theory and experiment that are slightly higher when using the smaller 4-31G basis set than for the neutral species previously discussed. The larger 6-31G* basis set provides frequencies which, on average, exhibit differences similar to those observed for the neutral molecule. Here, the agreement between theory and experimental band positions is generally within 10–20 cm^{-1} . A larger basis set does not appear to keep the discrepancy between the experimental integrated intensity and the calculated value from increasing. This discrepancy is three times higher than that observed for the neutral calculation, regardless of the basis set utilized. There is another interesting thing to note regarding the band intensity calculations. In general, for the neutral as well as the cation, the calculated intensity is greater than that observed in the experiment. However, the experimentally observed bands at 1113.7, 1137.3 and 1243.0 cm^{-1} exhibit intensities significantly greater than the calculations indicate (see Fig. 2). One could argue, and rightly so, that the position of the 1243.0 cm^{-1} band is very close to a photoproduct band produced upon photolysis of

the Ar/ NO_2 matrix. Indeed, this fact resulted in the pure argon matrix data being used to determine the band's integrated intensity. Likewise, using the larger 6-31G* basis set, the B3LYP calculation did not produce a band around this frequency. Thus the intensity of this feature is suspect. This does not explain the discrepancy with the two remaining bands, 1113.7 and 1137.3 cm^{-1} . Although these bands are close to the region mentioned by Mattioda et al. (2003) as being dominated by the CN stretching and CNC in-plane bending modes, analysis of the theoretical results indicate these bands are primarily C–H in-plane motions. As discussed in Section 3.1, these fall in the interstellar emission region near the 8.6 μm feature.

A summary of band intensities for the CH out-of-plane bending region (1000–500 cm^{-1} or 10–20 μm) as well as the CC and CN stretching and CH in-plane bending modes (1500–1000 cm^{-1} or 6.7–10 μm) can be found at the bottom of Table 2. Since, typically, only 10–15% of the sample is converted into ions, theoretical values have also been included in the summary in order to prevent the potential oversight of any cation modes in the experimental results. From an earlier study of mono-substituted PANHs, Mattioda et al. concluded that, on average, the theoretical CH out-of-plane bending modes increase in intensity approximately 40% over those modes observed in the neutral PANH. This is almost identical to the increase in intensity observed in a non-substituted PAH. Dual substitution of the PANH does not appear to change this observation. Theoretical values for phenazine provide an increase in intensity of 32% for the CH out-of-plane bending modes following ionization. Experimental results are significantly lower than the theoretical values. This is probably due to the low concentration of cations in the sample and the inherent weakness of the CH out-of-plane bending modes to those of the CC and CN stretching and CH in-plane bending modes. Interestingly the experimental data for anthracene results in an even lower value for the cation to neutral ratio. The mono-substituted PANHs exhibit an approximate 10-fold increase in intensity for the CC and CN stretching and CH in-plane bending modes upon ionization (Mattioda et al., 2003). This compares to a 20-fold increase observed for a non-substituted PAH. However, as reported in Mattioda et al., given that a mono-substituted neutral PANH already exhibits a 2 fold increase in intensity for this region over an unsubstituted PAH, the overall increase in intensity remains approximately the same for a PANH cation over a neutral PAH. The addition of a second nitrogen to a PANH cation appears to result in a further enhancement of the CC and CN stretching and CH in-plane bending region. This is demonstrated in Table 2,

Table 2

Theoretical and experimental band positions, relative (RI) and integrated (km/mol) intensities and symmetry assignments (Sym) for the phenazine cation and experimental band positions and relative intensities for the anthracene cation

Phenazine cation										Anthracene cation							
Experiment					Theory					Experiment vs. theory $\Delta\%$							
					4-31G basis set		Sym	6-31G* basis set		4-31G basis set		6-31G* basis set					
ν (cm^{-1})	λ (μm)	RI	A	Comment	ν (cm^{-1})	A			ν (cm^{-1})	A	$\Delta\nu$ (%)	ΔA (%)	$\Delta\nu$ (%)	ΔA (%)	ν (cm^{-1})	RI	A
567.0	17.64	0.09	36.9		587.1	36.4	B2U	570.8	47.4	3.55	1.48	0.67	28.2				
723.0	13.83	0.02	7.2	Side bands 724.537, 727.163													
755.5	13.24	0.14	57.2	Side bands 756.686, 758.485	767.8	150.0	B3U	758	119.8	1.62	162.40	0.33	109.4	748.3	0.26	40.9	
826.4	12.10	0.03	12.1		817.1	67.3	B2U	825.4	73.1	1.13	454.01	0.12	501.4				
841.2	11.89	0.02	7.5														
897.9	11.14	0.01	2.2		887.4	9.6	B1U	886.6	11.3	1.16	326.48	1.25	403.5	912	0.09	14.4	
1022.5	9.78	0.02	8.3		1005.7	11.3	B2U	1015.5	10.9	1.64	36.15	0.69	31.9				
1113.7	8.98	0.02	6.6		1112.9	0.4	B1U	1115.3	0.0	0.07	94.33	0.14	99.8				
1137.3	8.79	0.16	66.7	Doublet with 1138.727	1163.1	12.6	B2U	1149.7	35.3	2.27	81.11	1.09	47.1	1183.3	0.01	2.2	
1243.0	8.04	0.04	38.8	Side band 1246.435, data from Ar	1249.3	1.2	B1U			0.51	96.89			1188.6	0.70	108.4	
1264.6	7.91	0.01	5.3														
1276.1	7.84	0.82	344.9		1257.1	728.8	B2U	1269.4	609.9	1.49	111.28	0.53	76.8				
1281.8	7.80	0.01	5.5										100.0				
1295.9	7.72	0.01	6.1		1298.7	1.2	B1U	1302.6	0.1	0.21	80.05	0.52	98.9	1290.4	0.06	9.0	
1309.5	7.64	0.02	6.9														
1315.4	7.60	0.03	13.7	Complex with 1314.241										1314.6	0.06	9.0	
1335.0	7.49	0.34	142.1	Shoulders 1331.631, 1333.530										1341	1.00	156.5	
1349.0	7.41	1.00	420.3	Complex with 1345.973, 1351.619	1349.2	235.5	B2U	1367.8	458.0	0.02	43.97	1.40	9.0	1352.6	0.31	48.2	
1361.3	7.35	0.14	58.4	Side band 1365.811	1373.2	175.7	B2U	1380.7	62.3	0.87	200.92	1.42	6.8	1364.4	0.04	6.0	
1389.2	7.20	0.01	4.1											1406.1	0.02	2.3	
1452.4	6.89	0.02	9.9	Side bands 1448.191, 1455.681										1409.5	0.11	16.3	
1464.5	6.83	0.03	13.2		1460.4	59.1	B1U	1463.3	54.0	0.28	347.57	0.08	308.7	1418.4	0.86	132.4	
1494.6	6.69	0.08	32.6		1484.3	70.6	B2U	1499.9	110.9	0.69	116.39	0.36	239.9	1430.2	0.01	2.3	
1519.4	6.58	0.01	5.1											1456.5	0.07	11.4	
1577.2	6.34	0.02	10.5											1539.9	0.15	23.5	
1590.0	6.29	0.08	31.8	Intensity might be enhanced by a water band	1559.8	48.6	B1U	1580	45.9	1.90	52.75	0.63	44.3	1586.4	0.14	21.7	
2487.7	4.02	0.01	5.6	Complex with 2470.566, 2477.583, 2493.595													
2516.1	3.97	0.01	5.6														
2540.2	3.94	0.01	5.8														
2734.2	3.66	0.03	12.6	Side band 2740.512													
2763.3	3.62	0.02	6.8														
2934.1	3.41	0.02	10.2	Doublet with 2928.027													
3055, 3078, 3095, 3110	3.27, 3.25, 3.23, 3.22	0.02	6.6		3092, 3099, 3107, 3113	10.5		3090, 3103, 3017	7.0								
Previous PANH results			123.2	Sum 500–100		263.3			251.4	Average differences (%)							55.4
Singly Substituted			1188.6	Sum 1000–1500		1296.5			1341.4	1.16	147.05	0.66	140.4				527.6
			2.2	Phenazine/anthracene 500–1000		4.8			4.5								
			2.3	Phenazine/anthracene 1000–1500		2.5			2.5								
				Experimental results													
PANH+/PANH		(1.41)	0.7	Phenazine cation/neutral 500–1000		1.3			1.5								
PANH+/PANH		(9.60)	15.5	Phenazine cation/neutral 1000–1500		14.4			22.0								

Differences between theoretical and experimental values are provided as percent difference ($\Delta\%$). Average differences are for the 500–1500 cm^{-1} range. Data truncated at the 1% relative intensity level.

Table 3
Theoretical and experimental band positions, relative intensities (RI) and symmetry assignments (Sym) for the phenazine anion

Phenazine anion					Theory				Theory vs. experiment				
Experimental					4-31G basis set		Sym	6-31G*basis set		4-31G basis set		6-31G*basis set	
ν (cm^{-1})	λ (μm)	R.I.	A (km/mol)	Comment	ν (cm^{-1})	A (km/mol)		ν (cm^{-1})	A (km/mol)	$\Delta\nu$ (%)	ΔA (%)	$\Delta\nu$ (%)	ΔA (%)
					610.6	2.5	B2U	600.0	3.2				
					659.3	1.2	B1U	653.7	1.1				
723.1	13.829	0.237	45.7	Side bands 724.537, 727.163	727.9	131.1	B3U	719.3	102.2	0.66	186.72	0.52	123.50
826.4	12.101	0.052	10.1		808.9	13.6	B2U	819.1	20.3	2.12	35.28	0.88	101.77
		0.000			867.4	9.3	B1U	862.9	11.9				
888.0	11.261	0.015	2.8		896.8	14.5	B3U	873.4	9.8	0.99	414.78	1.65	248.21
1018.2	9.821	0.028	5.4		1008.4	12.2	B2U	1018.1	13.4	0.96	126.49	0.01	148.58
1113.8	8.978	0.088	17.0		1110.8	14.8	B1U	1110.0	16.7	0.27	13.14	0.34	2.01
1137.3	8.792	0.041	7.8		1144.4	8.6	B2U	1132.2	0.6	0.62	9.87	0.45	92.20
1264.0	7.911	0.368	71.0		1251.4	325.4	B2U	1276.7	148.6	1.00	358.29	1.00	109.28
1309.6*, 1314.2	7.64*, 7.61	1.000	192.9	Doublet with 1315.39 shoulder	1296.0	263.2	B2U	1317.9	434.2	1.03	36.40	0.64	125.01
1333.2	7.501	0.135	26.0										
1519.0	6.583	0.027	5.3		1504.2	76.6	B2U	1525.6	80.0	0.97	1351.23	0.44	1415.97
1589.8	6.290	0.106	20.4		1570.6	1.7	B1U	1590.7	3.7				
2974.6	3.362	0.019	3.6										
3042.6	3.287	0.206	39.7	Broad weak complex	3006.8	19.2	B1U	3008.9	14.6				
3077.7	3.249	0.054	10.5		3026.2	162.2	B2U	3025.8	136.3				
					3048.3	158.2	B1U	3043.5	160.1				
					3054.9	121.3	B2U	3048.9	118.8				
			58.6	Anion Sum 500–1000		172.2				Average differences (%)			
			325.5	Anion Sum 1000–1500		700.8				0.96	281.36	0.66	262.95
			171.4	Neutral phenazine sum 500–1000		200.9							
			76.5	Neutral phenazine sum 1000–1500		89.7							
			0.3	Ratio anion/neutral 500–1000		0.9							
			4.2	Ratio anion/neutral 1000–1500		7.8							

Differences between theoretical and experimental values are provided as percent difference ($\Delta\%$). Average differences are for the 500–1500 cm^{-1} range. Data truncated at the 1% relative intensity level.

* Indicates major band of a multiplet.

the phenazine cation displays a 15-fold increase, both in theory and experimental observations, for the CC and CN stretching and CH in-plane bending region over the neutral dual substituted PANH. Surprisingly, the anthracene cation also displays a 14-fold increase for this region upon ionization, based on the experimental results. Given that phenazine already exhibits twice the intensity of anthracene for this region, this change in intensity implies that the CC and CN stretching and CH in-plane bending modes for the phenazine cation are double that of the unsubstituted anthracene cation. The experimental values in Table 2 confirm that this is indeed the case. The reader is cautioned that this is only one example of a dual substituted PANH. Further research is necessary to determine if this trend is true for all multiply substituted PANHs.

3.3. Phenazine anion

Fig. 2 displays the first reported theoretical and experimental spectrum of a PANH anion. The band positions and intensities for the phenazine anion are displayed in Table 3. As noted in the cation section, the larger basis set (6-31G*) exhibits a slightly better agreement with the experimental frequencies. Differences between the integrated intensities and the calculated values appear to be larger for the anion than observed for either the neutral or the cationic species. This larger discrepancy could be the result of the method used to determine anion concentration in the sample, a low anion concentration in the sample, resulting in a larger uncertainty in the integrated intensity, or due to the accuracy of the level of theory used in the calculation of intensities. More experiments and calculations are necessary to accurately determine the source of this increasing discrepancy. As with the cation calculations, both basis sets tend to overestimate the intensities of the bands, with the same two interesting exceptions. The anion bands at 1113.8 and 1137.3 cm^{-1} exhibit intensities that are equal to or greater than the calculated values (see Fig. 2).

The spectrum of the phenazine anion resembles that of the cation as well as the anthracene cation in that the CC and CN stretching and CH in-plane bending region exhibits much more intensity than the CH out-of-plane bending region. However, the ratio of the intensity for the CC and CN stretching and CH in-plane bending region for the anion is only four (experimental) to eight (theory) times that of the neutral PANH, compared to 15 times that for the cation. Both the experimental and theoretical results for the anion show a decrease in the CH out-of-plane region (1000–500 cm^{-1} or 10–20 μm) intensity compared to the neutral phenazine molecule. Since anthracene did not produce an apprecia-

ble amount of anion, it is impossible to compare with the phenazine anion.

4. Conclusions

The spectra of neutral, positively charged and negatively charged phenazine ($\text{C}_{12}\text{H}_8\text{N}_2$), isolated in an argon matrix, are presented. As with singly substituted PANHs, it appears that multiply substituted PANHs display increased intensity in the CC and CN stretching and CH in-plane bending modes when compared to the normal, unsubstituted PAHs. Upon ionization, the CC and CN stretching and CH in-plane bending modes of this multiply substituted PANH reveals an increase in intensity greater than that observed in a mono-substituted PANH. This report also includes the first mid-infrared spectrum of a PANH anion and the direct evidence of anion formation in a PANH molecule. It remains to be seen if the additional substitution of nitrogen into a PANH will result in further increase of the CC and CN stretching and CH in-plane bending modes beyond that found for this disubstituted PANH. The presence of additional nitrogen atoms in the PAH structure tends to enhance existing vibrational features rather than introduce new ones. Thus, it is possible for such nitrogen rich, biologically important, molecules to be present in interstellar objects exhibiting the PAH bands.

The use of a larger basis set results in a slight improvement in the calculated anion and cation frequencies. While, in general, the calculations tend to overestimate the intensities of the experimentally measured vibrational bands, there are two exceptions. The bands observed around 1113 and 1137 cm^{-1} exhibit intensities greater than or equal to the calculated intensities. Additional experiments are needed to determine the reason(s) why these C–H in-plane motions exhibit such behavior in the nitrogenated PAHs. Interestingly, these bands fall in the region of the interstellar 8.6 μm band and could contribute to the plateau emission long-ward of this feature.

Acknowledgments

This project was performed, in part, using compounds provided by the National Cancer Institute's Chemical Carcinogen Reference Standards Repository operated under contract by Midwest Research Institute, No. N02-CB-07008. The authors also wish to acknowledge the expert technical support of Bob Walker. Dr. Mattioda gratefully acknowledges the support of the National Research Council's Research Associateship Program. This work was fully supported by NASA's

Long Term Space Astrophysics and Exobiology programs, under Grants #399-20-0-05 and #344-58-3H.

References

- Bauschlicher, C.W., Langhoff, S.R. The calculation of accurate harmonic frequencies of large molecules: the polycyclic aromatic hydrocarbons, a case study. *Spectrochim. Acta A* 53, 1225–1240, 1997.
- Becke, A.D. Density-functional thermochemistry. III. The role of exact exchange. *J. Chem. Phys.* 98, 5648–5652, 1993.
- Cook, D.J., Saykally, R.J. Simulated infrared emission spectra of highly excited polyatomic molecules: a detailed model of the PAH-UIR hypothesis. *ApJ* 493, 793–802, 1998.
- Cox, P., Kessler, M.F. *The Universe as seen by ISO, Volume 2. ESA SP-427, ESTEC, ESAP Publications Division, Noordwijk, The Netherlands*, 1999.
- Durnick, T.J., Wait Jr., S.C. Vibrational spectra and assignments for phenazine. *J. Mol. Spectrosc.* 42, 211–226, 1972.
- Frisch, M.J., Pople, J.A., Binkley, J.S. Self-consistent molecular orbital methods. 25. Supplementary functions for Gaussian basis sets. *J. Chem. Phys.* 80, 3265–3269, 1984, and references therein.
- Frisch, M.J., Trucks, G.W., Schlegel, H.B., Gill, P.M.W., Johnson, B.G., Robb, M.A., Cheeseman, J.R., Keith, T., Peterson, G.A., Montgomery, J.A., Raghavachari, K., Al-Laham, M.A., Zakrzewski, V.G., Ortiz, J.V., Foresman, J.B., Cioslowski, J., Stefanov, B.B., Nanyakkara, A., Challacombe, M., Peng, C.Y., Ayala, P.Y., Chen, W., Wong, M.W., Andres, J.L., Replogle, E.S., Gomperts, R., Martin, R.L., Fox, D.J., Binkley, J.S., Defrees, D.J., Baker, J., Stewart, J.P., Head-Gordon, M., Gonzalez, C., Pople, J.A. *Gaussian 98, Revision A.11. Gaussian, Inc., Pittsburgh, PA*, 1998.
- Garrison, A.A., Mamantov, G., Wehry, E.L. Analysis of polycyclic aromatic compounds containing nitrogen and oxygen by matrix isolation Fourier transform infrared spectroscopy. *Appl. Spectrosc.* 36, 348–352, 1982.
- Hudgins, D.M., Allamandola, L.J. Infrared spectroscopy of matrix-isolated polycyclic aromatic hydrocarbon cations 2: the members of the thermodynamically most favorable series through coronene. *J. Phys. Chem.* 99, 3033–3046, 1995.
- Hudgins, D.M., Allamandola, L.J. Polycyclic aromatic hydrocarbons and infrared astrophysics: the state of the PAH model and a possible tracer of nitrogen in carbon-rich dust. in: *Astrophysics of Dust*. in: Witt, A.N., Clayton, G.C., Draine, B.T. (Eds.), *ASP Conference Series*, vol. 309, pp. 665–688, 2004.
- Hudgins, D.M., Bauschlicher Jr., C.W., Allamandola, L.J., Fetzer, J.C. Infrared spectroscopy of matrix-isolated polycyclic aromatic hydrocarbon ions. 5. PAHs incorporating a cyclopentadienyl ring. *J. Phys. Chem. A* 104, 3655–3669, 2000.
- Hudgins, D.M., Bauschlicher Jr., C.W., Allamandola, L.J. Variations in the peak position of the 6.2 μm PAH emission feature: a tracer of N in the interstellar PAH population. *ApJ*, in press, 2005.
- Hudgins, D.M., Sandford, S.A., Allamandola, L.J. Infrared spectroscopy of polycyclic aromatic hydrocarbon cations I: matrix-isolated naphthalene and perdeuterated naphthalene. *J. Phys. Chem.* 98, 4243–4253, 1994.
- Hudgins, D.M., Sandford, S.A. Infrared spectroscopy of matrix-isolated polycyclic aromatic hydrocarbons. 1. PAHs containing 2 to 4 rings. *J. Phys. Chem.* 102, 329–343, 1998.
- Kuan, Y., Charnley, S.B., Huang, H.C., Tseng, W.L., Kisiel, Z. Interstellar glycine. *ApJ* 593, 848–867, 2003.
- Mattioda, A.L., Hudgins, D.M., Bauschlicher Jr., C.W., Rosi, M., Allamandola, L.J. Infrared spectroscopy of matrix-isolated polycyclic aromatic hydrocarbons, 6. Polycyclic aromatic nitrogen heterocycles and their cations. *J. Phys. Chem. A* 107, 1486–1498, 2003.
- Neto, N., Ambrosino, F., Califano, S. Vibrational assignment of phenazine and phenazine-d8: crystal spectra in polarized light and force constants calculations. *Spectrochim. Acta* 20, 1503–1516, 1964.
- Oomens, J., van Roij, A., Meijer, G., von Helden, G. Gas-phase infrared photodissociation spectroscopy of cationic polyaromatic hydrocarbons. *ApJ* 542, 404–410, 2000.
- Peeters, Z., Botta, O., Charnley, S.B., Ruiterkamp, R., Ehrenfreund, P. The astrobiology of nucleobases. *ApJ* 593, L129–L132, 2003.
- Piest, J.A., von Helden, G., Meijer, G. Infrared spectroscopy of jet-cooled cationic polyaromatic hydrocarbons: naphthalene⁺. *ApJ* 520, L75–L78, 1999.
- Piest, J.A., Oomens, J., Bakker, J., von Helden, G., Meijer, G. Vibrational spectroscopy of gas-phase neutral and cationic phenanthrene in their electronic groundstates. *Spectrochim. Acta A* 57, 717–735, 2001.
- Pizzarello, S. Soluble organics in the Tagish lake meteorite: a preliminary assessment. 32nd Annual Lunar and Planetary Science Conference, March 12–16, 2001, Houston, TX, abstr. no. 1886, 2001.
- Ricca, A., Bauschlicher, C.W., Bakes, E.L.O. A computational study of the mechanisms for the incorporation of a nitrogen atom into polycyclic aromatic hydrocarbons in the Titan Haze. *Icarus* 154, 516–521, 2001.
- Schlemmer, S., Cook, D.J., Harrison, J.A., Wurfel, B., Chapman, W., Saykally, R.J. The unidentified interstellar infrared bands: PAHs as carriers?. *Science* 265, 1686, 1994.
- Stammer, C., Taurins, A. Infrared spectra of phenazines. *Spectrochim. Acta* 19, 1625–1653, 1963.
- Stephens, P.J., Devlin, F.J., Chabalowski, C.F., Frisch, M.J. Ab initio calculation of vibrational absorption and circular dichroism spectra using density functional force fields. *J. Phys. Chem.* 98, 11623–11627, 1994.
- Stoks, P.G., Schwartz, A.W. Basic nitrogen-heterocyclic compounds in the Murchison meteorite. *Geochim. Cosmochim. Acta* 46, 309–315, 1982.
- Szczepanski, J., Roser, D., Personette, W., Eyring, M., Pellow, R., Vala, M. Infrared spectrum of matrix-isolated naphthalene radical cation. *J. Chem. Phys.* 96, 7876–7881, 1992.
- Szczepanski, J., Vala, M. Electronic and vibrational spectra of matrix isolated anthracene radical cations: experimental and theoretical aspects. *J. Chem. Phys.* 98, 4494–4511, 1993.
- Wagner, D.R., Kim, H.S., Saykally, R.J. Peripherally hydrogenated neutral polycyclic aromatic hydrocarbons as carriers of the 3 micron interstellar infrared emission complex: results from single-photon infrared emission spectroscopy. *ApJ* 545, 854–860, 2000.